Hybridization of a sigma-delta-based CMOS hybrid detector

Kolb, K.E.[a]; Stoffel, N.C.[c], Douglas, B.[c]; Maloney, C.W.[a]; Raisanen, A.D.[b]; Ashe, B.[a]; Figer, D.F.[a]; Tamagawa, T.[d]; Halpern, B.[d]; Ignjatovic, Zeljko[e]

[a] Rochester Imaging Detector Lab, Rochester Institute of Technology, 54 Lomb Memorial Dr., 76-A230, Rochester, USA;
[b] Rochester Institute of Technology IT Collaboratory, 74 Lomb Memorial Dr., Rochester, USA;
[c]Infotonics Technology Center, 5450 Campus Dr., Canandaigua, USA
[d]Jet Process Corporation, 57B Dodge Avenue, North Haven, USA
[e]The University of Rochester, 500 Joseph C. Wilson Blvd., Rochester, USA

ABSTRACT

The Rochester Imaging Detector Laboratory, University of Rochester, Infotonics Technology Center, and Jet Process Corporation developed a hybrid silicon detector with an on-chip sigma-delta (ΣΔ) ADC. This paper describes the process and reports the results of developing a fabrication process to robustly produce high-quality bump bonds to hybridize a back-illuminated detector with its ΣΔ ADC. The design utilizes aluminum pads on both the readout circuit and the photodiode array with interconnecting indium bumps between them. The development of the bump bonding process is discussed, including specific material choices, interim process structures, and final functionality. Results include measurements of bond integrity, cross-wafer uniformity of indium bumps, and effects of process parameters on the final product. Future plans for improving the bump bonding process are summarized.

Key Words: Silicon Photodiode, Hybridization, Bump bonding, Lift-off Resist, Jet Vapor Deposition

1. INTRODUCTION

The purpose of the bump bond process developed is to bond a PIN silicon photodiode to a ΣΔ ADC ROIC (Analog to Digital Count Read-Out Integrated Circuit). The hybridized detector will have low noise, low power dissipation, low mass, and improved low-light response outperforming existing imagers. The ΣΔ ROIC has very low readout noise by design and will have the capability to address individual pixels during signal integration via CMOS (Complementary Metal Oxide Semiconductor field effect transistor) implementation. The bump bonding facilitates a short, direct connection from the integration nodes to the readout circuitry as opposed to long, parasitic wires connected via external packaging.

For optimum detector performance, the bump metal must have the correct dimensions, the alignment must be within 1μm to prevent shorts between nodes, and the bonds must be mechanically strong and defect-free. The process developed to attain the correct dimensions, alignment techniques, and bond strength characterization to ensure good electrical contact are discussed and results are provided for validation. Figure 1 below shows a cross section of the hybridized structure when bonded together as intended.

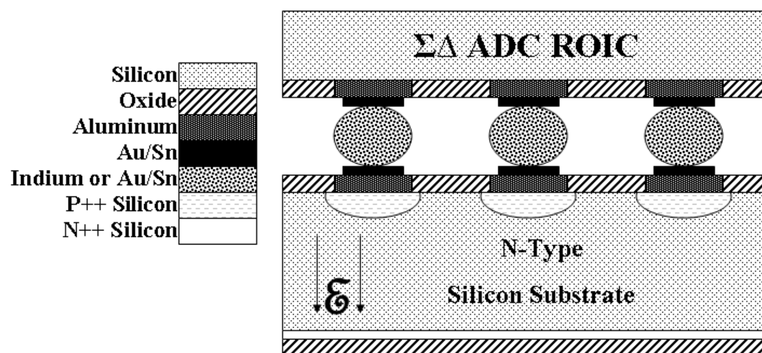

Figure 1. Hybridized Detector Architecture: Note the bump bonding structure of aluminum bonding pads, Intermetallic layer, and the indium or Gold/Tin bump bond in between.

2. APPROACH

To achieve the bonding structure, a sacrificial layer is used to define the size and shape of the deposited bump metal, and then a look-up/look-down optical system is used to align the ROIC and photodiode for bonding. Both of these processes entail multiple considerations and process accommodations to attain the desired results. The final metric for success of the entire process is the integrity of the bonds from the photodiode to ROIC. Figure 2 shows a flow chart of the steps involved in the process development from beginning to end.

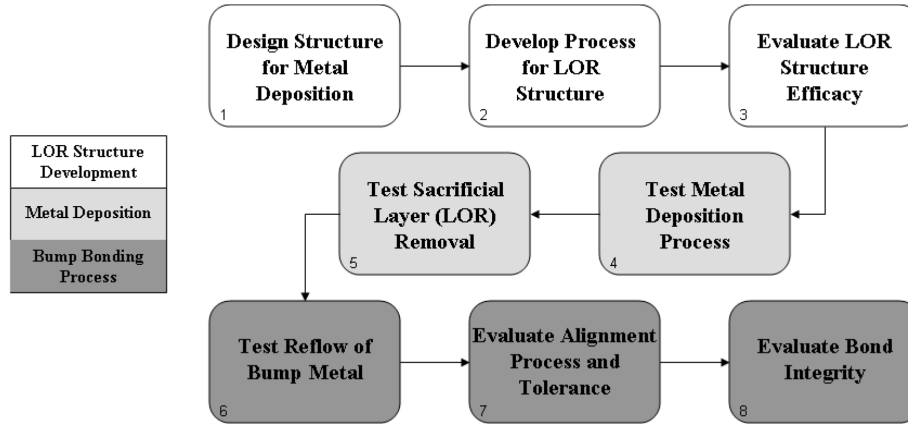

Figure 2. Flow chart for the development of the bump bonding process from start to finish; LOR is Lift-Off Resist, a polymer used in the structure that facilitates the shape of the deposited metal. Boxes 3, 5, and 8 will be discussed in Section 3.

2.1 LOR (Lift-Off Resist) Sacrifical Structure

The first step towards forming the metal bumps is to devise a structure or process that facilitates the formation of the desired pre-reflow (initial as-deposited) shape and size of the bump metal. Here, a process is developed that involves a lift-off resist (LOR) and photosensitive resist polymer sacrificial structure (a structure that only exists temporarily and is not present in the final device) that is used to produce the correct metal dimensions. Since the metal is deposited uniformly across the device, the polymer structure must have openings over the areas where the metal deposition is desired (over the integration node contacts). The structure must also be thicker than the uniformly deposited metal so that the metal layer becomes discontinuous over the openings. The designed structure can be seen in Figure 3.

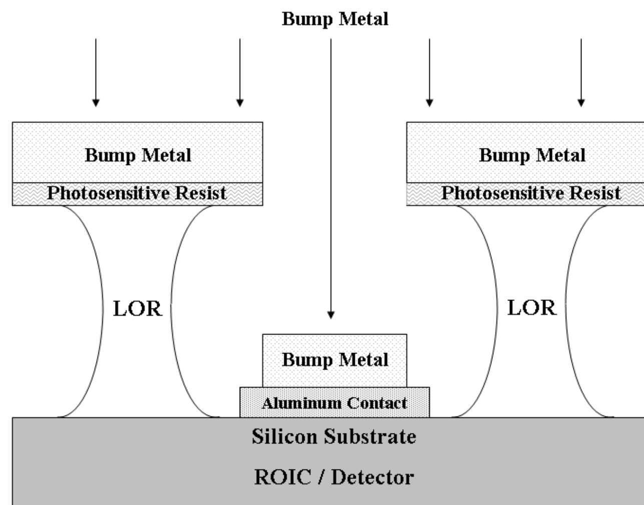

Figure 3. Diagram of the sacrificial LOR structure devised for the facilitation of localized metal deposition from a uniform deposition process (not to scale); Photosensitive Resist refers to a photosensitive polymer that allows for the patterning of the structure via lithography.

The structure in Figure 3 is achieved by a number of processing steps. First, a lift-off resist (Microchem LOR-30A) is coated over the entire device to a thickness of 4µm, which (when added to the thickness of the photosensitive resist) is thick enough to achieve discontinuity in the deposited metal layer over the opening in the structure (see Figure 3). Obtaining the correct thickness in the LOR layer requires a spin speed of 2000rpm for 45 seconds. The polymer must then be baked to strengthen the polymer chains, the temperature and length of which determines the etch rate of the material (a longer bake or higher bake temperature would decrease the etch rate of the material). The selection of these process parameters will be discussed later in context with the desired structure metrics and etch rate. For the photosensitive resist (FujiFilm HPR504) layer, a standard spin-on recipe of 2500rpm for 45 seconds, followed by a bake at 100°C for 90 seconds, gives a thickness of 1.3µm.

The shape of the structure is achieved by a succession of steps known as the photolithography process. The stack of polymers (LOR underneath a photosensitive resist layer) is exposed using mercury broadband light through a patterned mask, which causes a photochemical reaction, weakening the bonds of the photosensitive resist in any exposed areas. The weakened chains can then be removed using a liquid chemical developer. For the photosensitive resist, the developer only affects the exposed areas, leaving the unexposed areas intact. For the LOR layer, since it is not photosensitive, the developer acts as an isotropic etchant, meaning that it etches the material equally in all directions. The removal of exposed photosensitive resist and the etching of the LOR layer takes place in one step, the length of which is determined by the etch rate of the LOR and the profile desired for the final structure.

Using the LOR manufacturer's recommendations and a few preliminary tests, a bake temperature for the LOR of 170°C for 5 minutes was chosen. Figure 4 shows the diameter of the structure's key dimensions (LOR opening over the metal pads and the photosensitive resist opening), with respect to the time spent in developer (for the entire polymer stack).

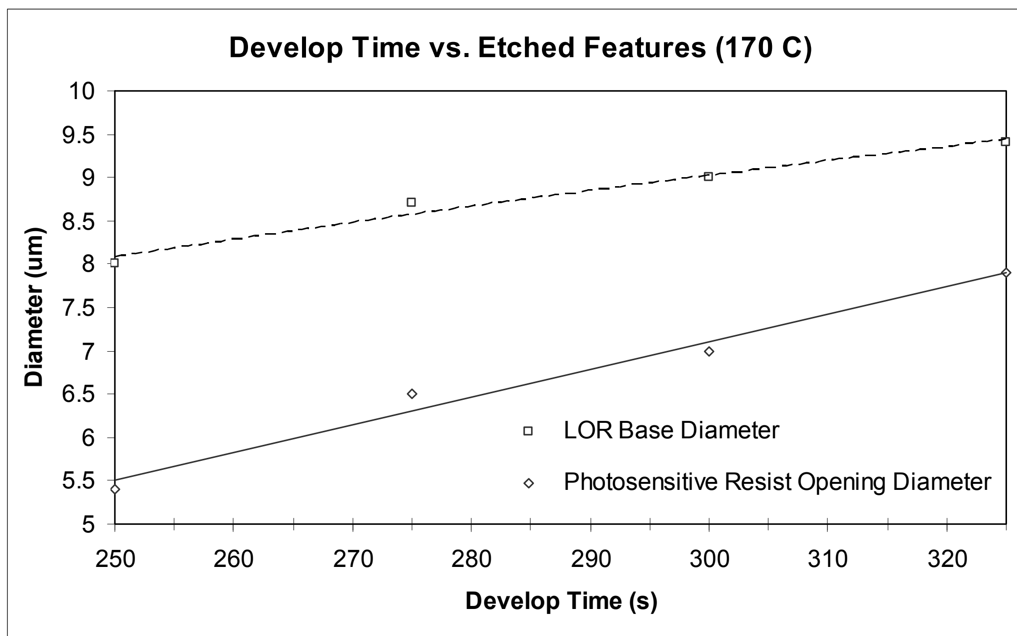

Figure 4. Designed experiment results for Etched Features vs. Development Time for the LOR profile. All points were processed at 170°C for 5 minutes. The linear slope shows that predictability exists within the parameters chosen and so the process point for these parameters can be chosen from this plot.

The difference in the diameter of the photosensitive resist opening with increasing development time is due to thickness loss, since the etching process in that material is not completely anisotropic (directionally or locally preferential). The process point of 270 seconds in the developer gives the desired dimensions: the desired opening over the Aluminum pad in the photosensitive resist is 6µm (defining the diameter of the deposited metal on the Aluminum pad) and the cleared opening at the bottom of the polymer structure must be greater than 6µm so that the constraining dimension is the photosensitive resist to avoid contamination of the metal surface with residual LOR (which would inhibit bond strength). See Figure 3 again for reference to the structure dimensions.

Figure 5 shows the preliminary results for the polymer structure on a non-device substrate, achieved with the process design discussed above. The efficacy of the structure can only be determined by the resulting effect it has on the shape and location of the deposited bump metal in the final device.

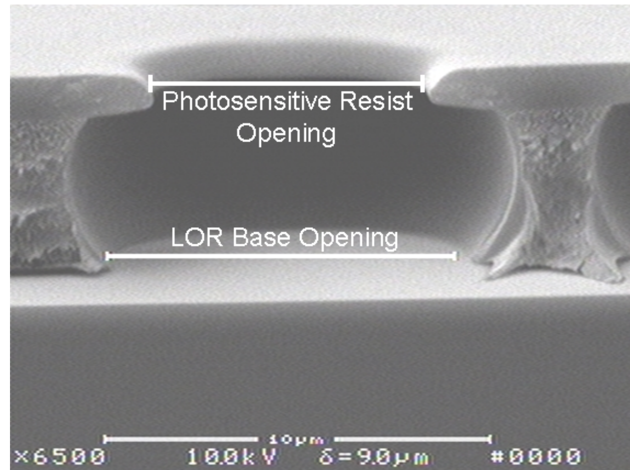

Figure 5. Preliminary results (non-device substrate) for the polymer structure, fabricated with the designed process discussed; The diameter of the photosensitive resist opening is 6.5µm, the diameter of the LOR base opening is 9µm, and the height of the full structure is 5.5µm. Image acquired with an SEM (Scanning Electron Microscope).

2.2 Metal Deposition[1,2]

For the bonding process, two different bump metals were chosen for investigation: Indium and Gold/Tin (AuSn). The advantage of Indium is its ductility, which is advantageous when materials of different coefficients of thermal expansion (CTEs) are bonded together because it absorbs the stress created in the bonds. Indium is also frequently used in imager bump bonding because it maintains its desirable properties under cryogenic conditions. The alternative, AuSn solder, is well-known with demonstrated reliability for optoelectronics and micro-electro-mechanical systems (MEMS) applications. While AuSn is a hard solder, in this application both the ROIC and photodiode substrates are made of Silicon, and therefore material CTE differences should have negligible impact.

A suitable method for depositing the Indium or AuSn (Gold/Tin) bumps in this application must operate at a low temperature compatible with organic materials (the polymer structure) and be capable of defining arrays of precisely shaped bumps in the micron size range at small pitch. Jet Vapor Deposition (JVD) satisfies these requirements.

In a basic JVD vapor source, Helium or Argon gas flows from an upstream region at pressures of several torr, through a restrictive opening, into a downstream region of pressure of about 1Torr. Low pressure, fast flow and “choked” flow conditions are sustained by a mechanical pump in series with a Roots blower (a positive displacement pump). This system produces a collimated jet of gas traveling at the speed of sound. For metal to enter this collimated jet of gas, it must first be vaporized (the approach for which changes based on the desired deposition metal). AuSn 80/20 (percent proportion) wire or ribbon is fed by a knurled wheel mechanism and vaporized from a hot Tungsten coil. Indium wire, however, is too soft to feed; instead, liquid Indium flows from a melt reservoir through a metal "wick" to a hot Tungsten filament from which it vaporizes. The metal atoms are vaporized upstream of the restrictive opening, enter into the collimated jet, and finally deposit onto the surface of the wafer downstream. The jet diameter (set by the restrictive opening) is 0.5-1.0cm, and the evaporated metal deposits within a circle of similar diameter with high capture efficiency. Because the deposition process is of a localized nature, uniform coating of a wafer requires movement so that every area of the wafer is processed equally. This can be done by spinning the wafer at a high revolution rate and scanning it slowly back and forth in front of the jet. Further discussion of JVD principles of operation, jet source designs, and relative motion schemes can be found in References 1 and 2.

Unlike other metal deposition techniques such as normal evaporation, the JVD process causes the evaporated metal atoms to bond together, and these nanoclusters have high enough energies to avoid deflection on impact with other atoms within the collimated jet of gas. This leads to a highly perpendicular trajectory at impact with the wafer, giving the process a highly isotropic nature and the ability to grow columns of metal from the surface of the wafer up with high

aspect ratios and flat tops (desirable for the bonding process). This ability to grow metal nanoclusters and deposit them at high rate to form dense arrays of fine pitch metal bumps is a key advantage of JVD for the present work[1].

2.3 Removal of Sacrificial Structure

After metal deposition, the photosensitive resist and LOR layers are stripped in PG Remover™ at 65°C for 12 hours. PG Remover™ is a commercial photoresist stripper by Microchem. Ultrasonics are commonly used to perturb the polymer and substrate during removal to aid in liftoff, but is not used in this application due to concerns about damaging the bump structures. The wafers are then rinsed with de-ionized water, and another layer of photoresist is applied over the Indium or AuSn bumps prior to singulation in a dicing saw. This protective photoresist is removed with acetone prior to bonding.

2.4 Bump Formation, Alignment, and Bond Integrity

The ROIC and photodiode devices are bonded together using an S.E.T. FC150 flip chip bonder, which is capable of 1µm post-bond placement accuracy and 20µrad planarity. The ROIC and photodiode are both held using vacuum tooling made from Silicon Carbide (SiC) polished to better than 2um flatness. Once loaded into the system the photodiode will be on the universal bond arm, 150mm above the ROIC (which is on the substrate chuck). The microscope stage is then positioned between the ROIC and photodiode and the devices are aligned and leveled using the look-up/look-down optical system. The upper bond arm then moves down into contact and the tool applies pressure (and in some instances, heat) to complete the bond.

After bonding, alignment is checked using infrared microscopy. The devices are then pulled apart and the failure mode is observed using optical microscopy. A good Indium-to-Indium bond will result in a characteristic “taffy pull” (ductile) failure that can be viewed optically (see Section 3.3 for a more in-depth discussion of evaluating mechanical integrity).

Indium has a melting point of 156.6C. It is generally bonded at room temperature, or slightly elevated temperatures with pressures on the order of $0.8^{kg}/_{mm^2}$ of Indium area. A eutectic gold composition of 80% gold, and 20% tin by weight has a melting point of 283°C. Bonding is generally eutectic, meaning that heat is applied to reach just beyond the melting point of the solder during bonding.

3. INITIAL RESULTS

3.1 Evaluation of the Efficacy of the Polymer Structure

The opening in the processed structure’s photosensitive resist (top layer) is about 7µm, which is as expected, as shown in Figure 6. The portion of the wafer shown in the SEM image has small misalignment, though the process is still within working boundaries.

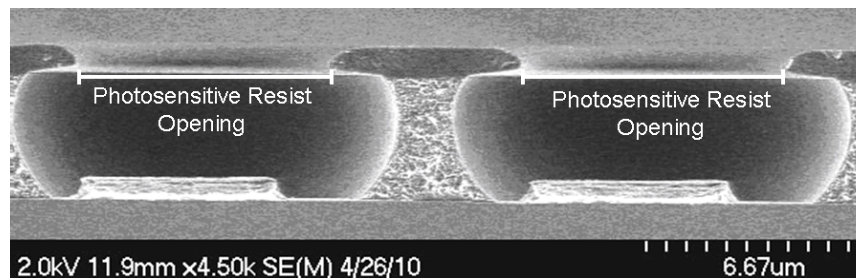

Figure 6. Polymer Structure before metal deposition. The structure appears as expected (see Figure 2), though slightly misaligned to the underlying metal pads.

3.2 Metal Deposition, Polymer Removal, and Reflow

Figure 7 shows identical polymer structures after metal deposition (one receiving AuSn and the other Indium). In both cases the resulting metal thickness is within 10% of the desired thickness. It appears that AuSn is the better choice for uniformity, and since the AuSn is reflowed, the final bump will be more uniform than the Indium.

During the initial metal deposition trial, a process failure occurred in which the photosensitive resist overhangs were absent (see Figure 7). Because these overhangs are missing, the shadowing effect illustrated in Figure 3 does not occur, leaving the metal to deposit across the entire bowl-shaped cavity created by the LOR isotropic etch profile. This is a failure jointly between the devised polymer structure and the method of metal deposition. It is probable that the JVD process is too energetic (with the nanoclusters of heavy metals bombarding the polymer structure), and therefore destroys the mechanically weak photoresist overhangs. Though the structure may be suited for less-energetic metal depositions, such as evaporation and sputtering, those processes lack the directionality that is so critical to defining the bump metal. The results of a different metal deposition process that lacks the directionality of the JVD process might yield results similar to those shown in Figure 7 due to the isotropic nature of the processes (and so would not be suitable). There are ways in which the polymer structure can be reinforced so that it can withstand the high energy of the JVD process, such as a change in materials used. These options will be discussed in Section 4.

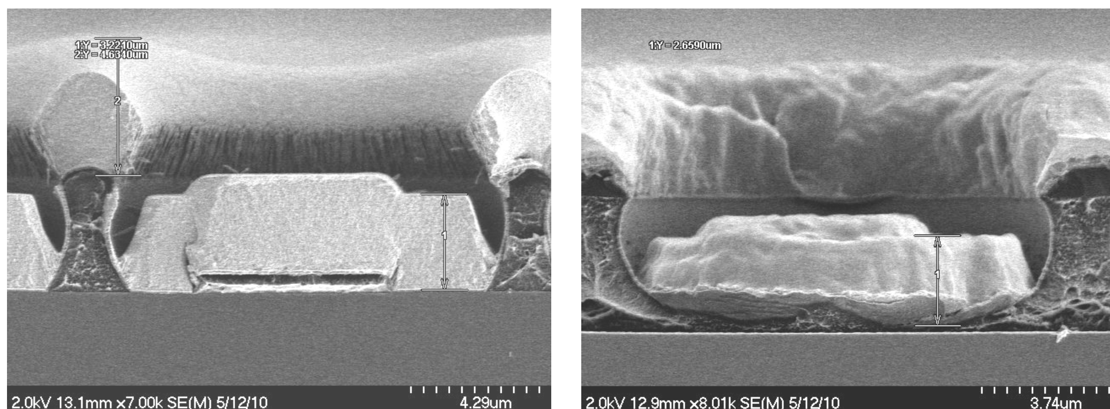

Figure 7. Polymer Structure after metal deposition. Left: AuSn deposition. The height of deposited metal is 3.2µm. Right: Indium deposition. The height of deposited metal is 2.7µm.

The AuSn and Indium bumps after liftoff of the LOR layer are shown in Figure 8. There is no visible residue from the polymer structure on the photodiode surface, indicating that the liftoff process successfully removed the LOR from the substrate.

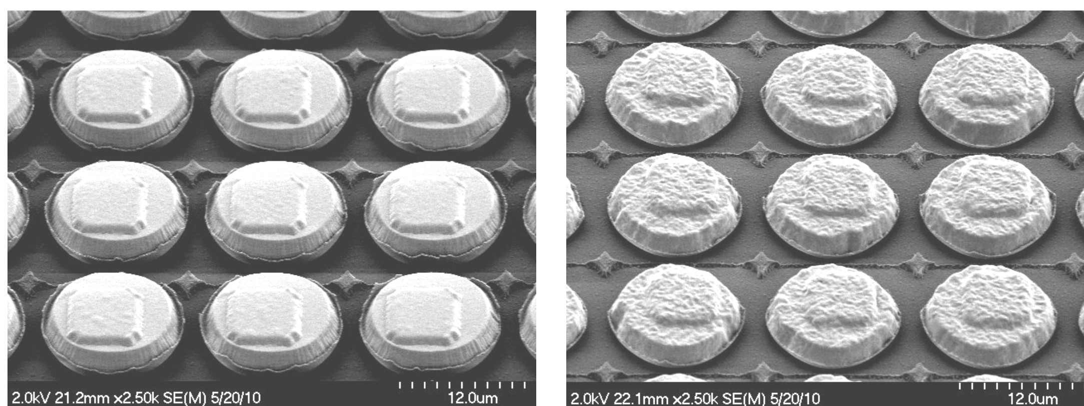

Figure 8. Left: Deposited AuSn after polymer removal, before reflow. Right: Deposited Indium after polymer removal. The polymer removal is very clean in both cases, though the over-sizing of the bumps is evident in the relief image of the underlying pad – the bump is meant to be roughly the size of the pad.

The AuSn bumps after the reflow process are shown in Figure 9. Although there is more mass than anticipated, the metal has still been smoothed to a rounded shape by the process. When the metal is properly shadowed by the overhangs in the polymer stack (resulting in less mass to heat and reform), the reflow process should render the bumps even smoother and cause them to have the expected spheroid shape. The indium bumps do not need a reflow step as the metal is soft enough to be suitable for bump bonding as-deposited.

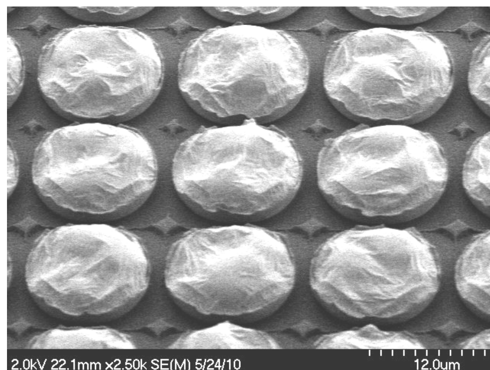

Figure 9. AuSn bumps after reflow of 15s at 310°C. There is irregularity in the surface of the bumps due to insufficient reflow of the extra mass deposited.

3.3 Bump Alignment and Bond Integrity

An infrared image of the aligned photodiode and ROIC is shown in Figure 10. Good alignment allows for proper bump to bump contact, which reduces the probability of two non-paired bumps merging under the bonding pressure. If any misalignment were present, the cross in the upper left of the image would appear to be doubled at the edges.

Figure 10. IR alignment image. The large cross structures (seen in the top left corner of the image) serve as alignment markers for the operator. These marks are present on all four corners of both the ROIC and photodiode device die.

Once alignment is achieved, the ROIC and photodiode die must be bonded together using force (and in some cases heat) so that the bumps on opposing pads can complete the connection. To determine the best possible force for bonding, a series of different forces were used until both a qualitatively and quantitatively good bond strength (characterized by the mode of failure and force required to separate the two devices, respectively) is achieved. The best bonding force for this size bump is 5kg.

The post-pull results of the initial bonding process are shown in Figure 11. Though there were intermittent "taffy pull"-type failures, the overall percentage of this failure mode was lower than desired. The presence of bump material left on the pads after the pull indicates that the weak point is not in the adhesion of the bumps to the bonding pads, but rather between the bumps. This is desired, as it facilitates ductile failures (the failure mode requiring the most force to achieve), but in this case the force required to break the bump-to-bump bond is lower than desired at 2.2kg.

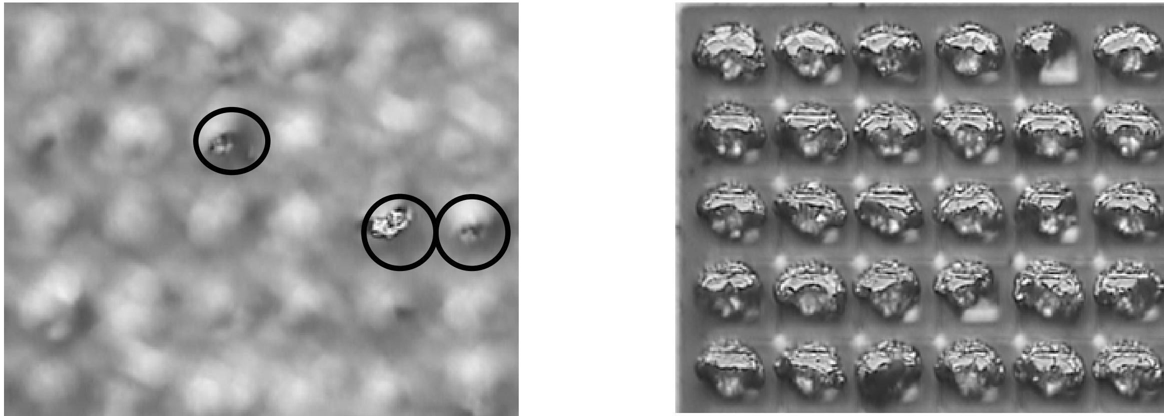

Figure 11. Pull test images. Left: Image with focus set above the plane of the bumps to highlight the ductile failures ("taffy pulls"); the circled features denote these ductile failures. Right: Image with focus set at bump plane to highlight the material left after pull (demonstrating that the failure occurred inside the bumps rather than at the interface between the bumps and the bonding pads). 5kg bond force and 2.2kg pull (separation) force.

4. FUTURE WORK

One item to address is the low mechanical strength of the photosensitive resist overhang structure. One possible solution to the destruction of these overhangs is to change the photosensitive material used in the top layer of the structure without altering the structure itself. Other polymers, such as SC-1827 (Dow Chemical), have more cross-linking (polymer chain bonding) and so have greater mechanical strength. Another advantage to such a polymer is the fact that it can be developed using a solvent, which does not affect the underlying LOR layer, and is also unaffected by the CD26 developer used to etch the LOR. This allows for independent processing of the bi-layer polymer structure, eliminating the thickness loss issues that had to be addressed when using the FujiFilm HPR504 photoresist. An alternative solution is to increase the thickness of the photosensitive resist layer, which increases the strength of the overhangs by decreasing the ratio of length to thickness and thereby increasing the amount of force necessary to break off the overhangs. A preliminary polymer structure utilizing the SC-1827 photosensitive resist is shown in Figure 12.

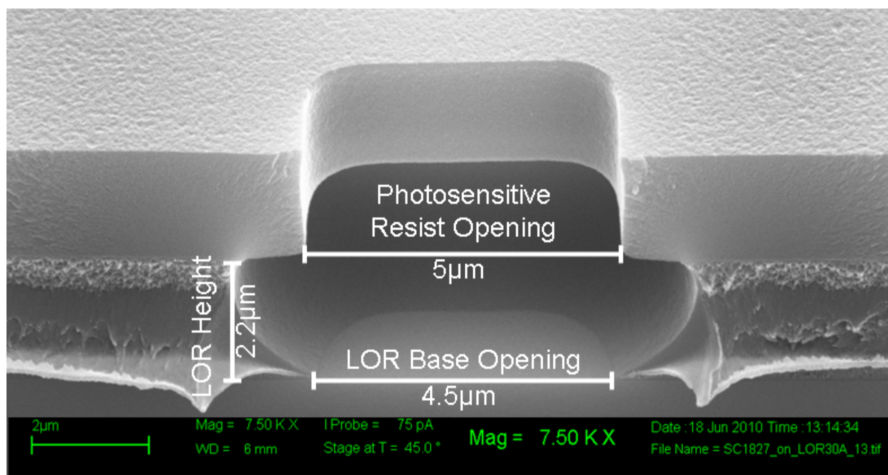

Figure 12. Preliminary polymer structure using LOR30A (Microchem) and SC-1827 (Dow Chemical). Dimensions are smaller than desired, but the structure can be tailored to the process specifications in further development.

Since the sacrificial polymer structure failed to shadow the areas underneath the overhangs, the mass of the resulting metal bumps are much higher than anticipated. This leads to reflow conditions that, while necessary to reflow bumps of the size obtained here, are not suitable for the desired bumps yet to be attained. This shortcoming in the initial process leads to the need for further process development of the reflow process. The same dilemma is also faced by the bonding portion of the process. Because the diameter of the bumps are larger than desired, combined with the pitch of the bumps themselves, merging of bumps occurs under pressures that would normally be required to bond the two sides together well. While the results from the alignment and bonding of the bumps in this instance is useful moving forward, the final conditions cannot be chosen until the metal bumps exhibit the correct dimensions.

ACKNOWLEDGMENTS

This material is based upon work supported by the National Aeronautics and Space Administration under Grant NNX07AG99G, issued through the Astronomy and Physics Research and Analysis Program of the Science Mission Directorate. Part of this research was performed in the Rochester Imaging Detector Laboratory and was supported by a NYSTAR Faculty Development Program grant for D. Figer.

The author would also like to thank Dr. Karl Hirschman, Christopher Shea, and Sean O'Brien, all of Rochester Institute of Technology, Rochester, NY, USA.

REFERENCES

(1) Gorski, Mike; Halpern, Bret. "Jet Vapor Deposition for AuSn Solder Applications". Advanced Packaging, February, 2003.
(2) Komarenko, Paul et. al. "Jet Vapor Deposition". Chapter 18 in Handbook of Deposition Technologies for Films and Coatings, 3rd Edition, edited by Peter Martin, Elsevier, 2009.
(3) Ignjatovic, Zeljko et. al. "Fully digital image sensor employing sigma-delta indirect feedback ADC with high-sensitivity to low-light illuminations for astronomical imaging applications". SPIE Conference Proceedings, Astronomical Telescopes and Instrumentation. June, 2010.